The 2010 IEEE/RSJ International Conference on
Intelligent Robots and Systems
October 18-22, 2010, Taipei, Taiwan

Trajectory Tracking of a Self-Balancing Two-Wheeled Robot Using Backstepping Sliding-Mode Control and Fuzzy Basis Function Networks

Ching-Chih Tsai, *Senior Member, IEEE*, Shang-Yu Ju, Shih-Min Hsieh, *Student Member, IEEE*

Abstract—This paper presents an adaptive backstepping sliding-mode motion controller using fuzzy basis function networks (FBFN) method for trajectory tracking of a self-balancing two-wheeled robot (SBTWR) with parameter variations. A decoupling method is proposed to decouple the robot's dynamic model such that the tracking controller can be synthesized using backstepping and sliding-mode control in both kinematic and dynamic levels. The FBFN is employed to on-line learn the uncertain parts of the tracking controller, thus achieving adaptive capability. Simulations results indicate that the proposed adaptive tracking controller is capable of providing satisfactory trajectory tracking performance.

Keywords: FBFN, sliding-mode control, trajectory tracking, wheeled inverted pendulum.

I. INTRODUCTION

Recently, self-balancing two-wheeled robots (SBTWRs), or called wheeled inverted pendulums, have been widely investigated in both academia and industry. Such robots have been successfully applied to construct several autonomous service robots [1-9]. Hosoda *et al.* [2] detailed the basic design of a human-symbiotic robot EMIEW whose linear motion speed was up to 1.67 m/sec; their EMIEW was designed based on a self-balancing two-wheeled structure. On the other hand, many researchers [3]-[9] have shown that the two-wheeled self-balancing platforms have gained many applications, including personal transportation vehicles, soccer games, service robots, and so on.

Modeling and control of the SBTWR have been widely studied by several researchers. Tsai et al. [3] proposed an adaptive neural network controller for a two-wheeled self-balancing mobile platform, but did not deal with trajectory tracking. Sasaki *et al.* [4] constructed a lightweight self-balancing personal riding-type wheeled mobile platform (PMP); the PMP steering control was achieved by changing the position of the rider's center of gravity. Grasser *et al*. [5] presented an unmanned mobile inverted pendulum, and Pathak *et al*. [6] studied the dynamic equations and control of the wheeled inverted pendulum by partial feedback linearization; however, they only addressed velocity control and position stabilization. Ha and Yuta [7] presented the trajectory tracking system for navigation of the inverse pendulum type self-contained mobile robot; however, this method was limited to simple straight line motion and simple turning.

From controller design of view, the control of the SBTWR can be thought of as an under-actuated control problem, which has been addressed by sliding-mode control approaches [10-11]. In particular, Lin and Mon [10] offered a hierarchical decoupling sliding-mode control to regulate a more general class of under-actuated control systems. Wang et al. [11] proposed two hierarchical sliding model control methods for the under-actuated control problem. However, the approaches [10-11] have not been applied to the SBTWR yet!

Recently, FBFNs have been adopted widely for nonlinear system modeling and control because they possess simple structure, good local approximating performance, particular resolvability, and function equivalence to a class of nonlinear function. Hence, FBFNs have been increasingly receiving attention in solving complex control problems. For example, Lin and Wang [12] presented FBFN-based robust self-tuning controller for robotic arms, Huaguang *et al.* [13] investigated an FBFN-based multivariable adaptive controller for nonlinear systems, and Lin [14] proposed an adaptive critic controller using FBFN for bank-to-turn missiles. Furthermore, Tsai *et al.* [3] employed similar FBFNs to approximate the unknown Coulomb and static frictions occurring in a two-wheeled self-balancing human transporter. However, the methods in [3, 14] have not been applied to the SBTWR with parameter variations and model uncertainties.

The goals of this paper are to propose an adaptive backstepping sliding-mode trajectory controller using FBFN to achieve trajectory tracking of the SBTWR in presence of parameter variations and model uncertainties, and to verify the controller by numerical simulations. The paper is written in two principal contributions; one is that a decoupling method is proposed to decouple the robot's dynamic model such that the motion controllers can be synthesized in both kinematic and dynamic levels; the other is the development of an adaptive trajectory tracking controller using FBFN.

The rest of the paper is outlined as follows. Section II decomposes the mathematical model of the SBTWR into two levels. Section III develops two backstepping sliding-mode controllers in both levels. In Section IV, the FBFNs are employed to on-line learn the uncertain parts of the controllers, thus achieving adaptive trajectory tracking. In Section V, simulation results are conducted to show the feasibility and effectiveness of the proposed control methods. Section VI concludes the paper.

Manuscript received March 3, 2010. This work was financially supported by the National Science Council, Taiwan, R.O.C., under the grant NSC 97-2221-E-005-070-MY3.

Ching-Chih Tsai (corresponding author), Shang-Yu Ju, Shih-Min Hsieh are with the Department of Electrical Engineering, National Chung Hsing University, 250 Kuo-Kuang Road, Taichung 40227, Taiwan, ROC. (corresponding author's e-mail: cctsai@nchu.edu.tw).

Table I. Parameters used for modeling and simulation.

Symbol and unit	Parameter and variable name	Value
I_{xx} , I_{yy} , I_{zz}	Moment of inertia of the pendulum body with respect to the x, y, z axis, respectively.	I_{xx} =2.1073 I_{yy} =1.8229 I_{zz} =0.649
v_r [m/sec]	Reference linear velocity	
ω_r [m/sec]	Reference angular velocity	
R [m]	Radius of both wheels	0.21
c_x, c_z	The center of mass of the vehicle is at Coordinate $OG_b = (c_x, 0, c_z)$ in β	C_z =0.21
τ_r , τ_l	Input torque applied to the right motor and the left motor	
I_{wa} , I_{wd} [$Kg\ m^2$]	Moment of inertia of a wheel about its axis and about a diameter respectively	I_{wa} =0.1563 I_{wd} =0.0781
ϕ_r , ϕ_l [rad]	angles of the right and left wheels	
θ [rad]	Yaw angle	
M_b [Kg]	Mass of the pendulum	70
M_w [Kg]	Mass of the each wheel	4
α [rad]	Tilt angle of the wheeled inverted pendulum	
b [m]	Half of the distance between both driving wheels	0.2
(x, y) [m/sec]	Position of the wheeled inverted pendulum	
v, ω	linear and angular velocities of the wheeled inverted pendulum	

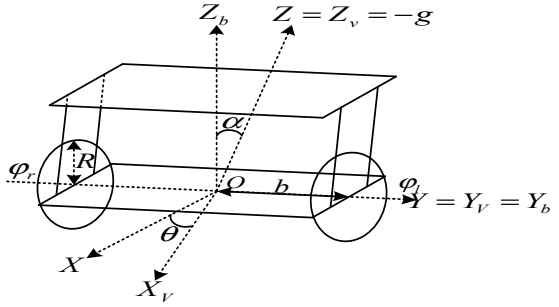

Fig.1. Free body diagram of the SBTWR.

II. SYSTEM MODELING AND DECOMPOSITION

2.1 Mathematical Modeling: Revisited

To steer the SBTWR, it is necessary to have its mathematical model such that a motion controller can be successfully designed based on the model in order to achieve desired control goals. Fig. 1 shows the free body diagram of the SBTWR whose mathematical model has been established in detail in [6]. In order to briefly recall the SBTWR's dynamic model, Table 1 lists all the used symbols and their definitions. With the symbols in Table 1 and the Euler-Lagrange equation, the dynamic model of the SBTWR was described in [2].

To simply the model, one defines the following notation and the augmented vector **x**,

$$\mathbf{q_r} = \begin{bmatrix} x & y & \theta & \alpha \end{bmatrix}^T,\ \mathbf{V} = \begin{bmatrix} \dot{\alpha} \\ v \\ \dot{\theta} \end{bmatrix} = \begin{bmatrix} \omega_\alpha \\ v \\ \omega \end{bmatrix},\ \mathbf{x} = \begin{bmatrix} \mathbf{q_r} \\ \mathbf{V} \end{bmatrix} \tag{1}$$

Thus,the state equation of the SBTWR is thus given by

$$\dot{\mathbf{x}} = f(\mathbf{x}) + \mathbf{g}(\mathbf{x})\mathbf{u} \tag{2}$$

where

$$\mathbf{f}(\mathbf{x}) = \begin{bmatrix} \mathbf{f_1}(\mathbf{x}) \\ \mathbf{f_2}(\mathbf{x}) \end{bmatrix}, \mathbf{g}(\mathbf{x}) = \begin{bmatrix} \mathbf{g_1}(\mathbf{x}) \\ \mathbf{g_2}(\mathbf{x}) \end{bmatrix}, \mathbf{u} = \begin{bmatrix} \tau_r \\ \tau_l \end{bmatrix}\ \mathbf{g_1}(\mathbf{x}) = \mathbf{0}_{4\times 2};$$

$$\mathbf{g_2}(\mathbf{x}) = \begin{bmatrix} g_{21}(\mathbf{x}) & g_{21}(\mathbf{x}) \\ g_{22}(\mathbf{x}) & g_{22}(\mathbf{x}) \\ g_{23}(\mathbf{x}) & -g_{23}(\mathbf{x}) \end{bmatrix} = \begin{bmatrix} \frac{1}{D_\alpha}(M_b R^2 + 2M_w R^2 + 2I_{wa} + M_b \cos(\alpha) c_z R) & \frac{1}{D_\alpha}(M_b R^2 + 2M_w R^2 + 2I_{wa} + M_b \cos(\alpha) c_z R) \\ -\frac{R}{D_\alpha}(M_b \cos(\alpha) c_z R + I_{yy} + M_b c_z^2) & -\frac{R}{D_\alpha}(M_b \cos(\alpha) c_z R + I_{yy} + M_b c_z^2) \\ \frac{R \cdot b}{G_\alpha} & -\frac{R \cdot b}{G_\alpha} \end{bmatrix}$$

$$\mathbf{f_1}(\mathbf{x}) = \begin{bmatrix} v\cos(\theta) & v\sin(\theta) & \dot{\theta} & \dot{\alpha} \end{bmatrix}^T$$

$$\mathbf{f_2}(\mathbf{x}) = \begin{bmatrix} f_{21}(\mathbf{x}) \\ f_{22}(\mathbf{x}) \\ f_{23}(\mathbf{x}) \end{bmatrix} = \begin{bmatrix} \frac{1}{D_\alpha}(\sin(2\alpha)\dot{\theta}\overline{H}) + \frac{1}{2D_\alpha}(M_b^2 c_z^2 R^2 \sin(2\alpha)(\dot{\alpha})^2) + \frac{1}{2D_\alpha}(-2M_b^2 R^2 c_z - 4I_{wa} M_b c_z - 4M_w R^2 M_b c_z) g \sin(\alpha) \\ K_\alpha \dot{\theta}^2 + \frac{1}{2D_\alpha}(M_b^2 c_z^2 R^2 g \sin(2\alpha)) + \frac{1}{4D_\alpha}(-4I_{yy} M_b R^2 c_z - 4R^2 M_b^2 c_z^3)\sin(\alpha)(\dot{\alpha})^2 \\ \frac{1}{G_\alpha}(-(I_{xx} - I_{yy})R^2 - M_b c_z^2 R^2)\sin(2\alpha)\dot{\alpha}\dot{\theta} - \frac{1}{G_\alpha}(\sin(\alpha) R^2 M_b c_z v\dot{\theta}) \end{bmatrix}$$

$$D_\alpha = M_b^2 \cos^2(\alpha) c_z^2 R^2 + ((-M_b^2 - 2M_w M_b) c_z^2 - 2I_{yy} M_w - I_{yy} M_b) R^2 - 2M_b c_z^2 I_{wa} - 2I_{yy} I_{wa}$$

$$G_\alpha = (-M_b c_z^2 + I_{zz} - I_{xx}) R^2 \cos^2(\alpha) + (M_b c_z^2 + I_{xx} + 2I_{wd} + 2b^2 M_w) R^2 + 2b^2 I_{wa}$$

$$K_\alpha (4D_\alpha) = (-4I_{yy} M_b R^2 c_z - 3R^2 M_b^2 c_z^3 + M_b R^2 c_z (I_{xx} - I_{yy}))\sin(\alpha) + (M_b R^2 c_z (I_{xx} - I_{zz}) + R^2 M_b^2 c_z^3)\sin(3\alpha)$$

$$\overline{H} = \frac{1}{2} M_b R^2 I_{zz} + I_{wa} I_{zz} - M_w R^2 I_{xx} - I_{wa} I_{xx} - M_b c_z^2 M_w R^2 - M_b c_z^2 I_{wa} - \frac{1}{2} M_b R^2 I_{xx} + M_w R^2 I_{zz}$$

2.2 Model Decomposition

With the transformation of the torques C_y and C_θ into the wheel torques τ_l and τ_r, one obtains

$$\mathbf{u} = \begin{bmatrix} \tau_l \\ \tau_r \end{bmatrix} = \begin{bmatrix} 0.5 & 0.5 \\ 0.5 & -0.5 \end{bmatrix} \begin{bmatrix} C_\theta \\ C_y \end{bmatrix} \tag{3}$$

and

$$\dot{\mathbf{V}} = \begin{bmatrix} f_{21}(\mathbf{x}) \\ f_{22}(\mathbf{x}) \\ f_{23}(\mathbf{x}) \end{bmatrix} + \begin{bmatrix} g_{21}(\mathbf{x}) & 0 \\ g_{22}(\mathbf{x}) & 0 \\ 0 & g_{23}(\mathbf{x}) \end{bmatrix} \begin{bmatrix} C_\theta \\ C_y \end{bmatrix} \tag{4}$$

From (2) and (4), it follows that the dynamic model of the SBTWR is decomposed into two levels of equations: kinematic and dynamic.

$$\dot{\mathbf{q}}_r = \begin{bmatrix} \dot{x} & \dot{y} & \dot{\theta} & \dot{\alpha} \end{bmatrix}^T = \begin{bmatrix} v\cos\theta & v\sin\theta & \omega & \omega_\alpha \end{bmatrix}^T \tag{5}$$

and

$$\dot{\mathbf{V}}_r = \begin{bmatrix} \dot{\omega}_\alpha \\ \dot{v} \\ \dot{\omega} \end{bmatrix} = \begin{bmatrix} f_{21}(\mathbf{x}) \\ f_{22}(\mathbf{x}) \\ f_{23}(\mathbf{x}) \end{bmatrix} + \begin{bmatrix} g_{21}(\mathbf{x}) & 0 \\ g_{22}(\mathbf{x}) & 0 \\ 0 & g_{23}(\mathbf{x}) \end{bmatrix} \begin{bmatrix} C_\theta \\ C_y \end{bmatrix} \tag{6}$$

The kinematic level reveals the relations between the position, orientation and inclination of the SBTWR and

their velocities, whereas the dynamic level involves with the relations between the three accelerations and the two torques, C_θ and C_y . Furthermore, from (5) and (6), it indicates that two controllers for C_θ and C_y can be synthesized independently from each other and then combined together to accomplish the control goal.

III. TRAJECTORY TRACKING

3.1 Problem Statement

The design goal of the trajectory tracking for the robot model described by (5) and (6) is to keep the trajectories of the SBTWR asymptotically follow time-varying reference trajectories, and to main the tilt angle of the pendulum at origin. To formulate the problem, let $\tilde{x}(t)$, $\tilde{y}(t)$, $\tilde{\theta}(t)$ be the differences between the real position $x(t)$, $y(t)$ and the angle $\theta(t)$ of the nonholonomic mobile robot with the desired reference trajectory, $\mathbf{q}_r(t)=[x_r(t), y_r(t), \theta_r(t)]^T \in R^3$, in the Cartesian coordinate, i.e.,

$$\tilde{x}(t)=x_r(t)-x(t),\ \tilde{y}(t)=y_r(t)-y(t),\ \tilde{\theta}(t)=\theta_r(t)-\theta(t) \quad (7)$$

Moreover, the desired reference trajectory $q_r(t)$ satisfies the following kinematics equation.

$$\dot{x}_{rc}(t)=v_r(t)\cos(\theta_r),\ \dot{y}_{rc}(t)=v_r(t)\sin(\theta_r),\ \dot{\theta}_r=\omega_r(t) \quad (8)$$

where $v_r(t)$ and $\omega_r(t)$ represents the desired time varying linear and angular velocities.

The aim of the trajectory tracking control method is to design two control laws for the two torques, C_θ and C_y, such that $\tilde{x}(t)\to 0, \tilde{y}(t)\to 0, \tilde{\theta}(t)\to 0$ as $t\to\infty$ and the inclination α is eventually maintained at zero.

3.2 Design of Trajectory Tracking Controller

The trajectory tracking controller of the SBTWR can be synthesized using backstepping in both kinematic and dynamic levels. In the kinematic level, two virtual controls for trajectory tracking are respectively constructed. In the dynamic level, the controlled torque vector to drive two wheels is established using the sliding-mode control approach, in order to achieve trajectory tracking.

3.2.1 Kinematic Level

For the kinematic part (5), the three variables $v(t)$, $\omega(t)$ and $\omega_\alpha(t)$ are regarded as virtual controls. To stabilize the inclination of the vehicle, it is easy to propose the virtual control

$$\omega_\alpha(t)=\phi_1(\alpha)=-k_\alpha\alpha, k_\alpha\in R>0 \quad (9)$$

so as to regulate the tilt angle to zero exponentially. On the other hand, to achieve

$$\tilde{x}(t)\to 0, \tilde{y}(t)\to 0, \tilde{\theta}(t)\to 0 \text{ as } t\to\infty \quad (10)$$

in the kinematic level, one considers the first three equations of the subsystem (5) as a well-known kinematic model of a mobile robot with differential driving, and applies the subsequent kinematic control approach to achieve the trajectory tracking goal. Since the errors between the actual and desired postures $\tilde{x}$, $\tilde{y}$, $\tilde{\theta}$ are defined in (7), the tangential error $e_1(t)$, the normal error $e_2(t)$ and the orientation error $e_3(t)$ is then obtained from the following matrix:

$$\begin{bmatrix} e_1(t) \\ e_2(t) \\ e_3(t) \end{bmatrix} = \begin{bmatrix} \cos\theta & \sin\theta & 0 \\ -\sin\theta & \cos\theta & 0 \\ 0 & 0 & 1 \end{bmatrix} \begin{bmatrix} \tilde{x} \\ \tilde{y} \\ \tilde{\theta} \end{bmatrix} \quad (11)$$

Differentiating the error vector obtains

$$\begin{cases} \dot{e}_1 = \omega e_2 - v + v_r\cos e_3 \\ \dot{e}_2 = -\omega e_1 + v_r \sin e_3 \\ \dot{e}_3 = \omega_r - \omega \end{cases} \quad (12)$$

Notice that the transformed errors, $e_1(t)$ $e_2(t)$ and $e_3(t)$, are continuous and bounded, the original errors, $\tilde{x}$, $\tilde{y}$, $\tilde{\theta}$ are bounded and continuous. Define a new auxiliary variable $\bar{e}_3(t)$:

$$\bar{e}_3(t)=e_3+\alpha e_2 \quad (13)$$

where $\alpha\neq 0$ .Taking the time derivative of $\bar{e}_3(t)$ yields:

$$\dot{\bar{e}}_3(t)=\dot{e}_3+k_3\dot{e}_2=\omega_r-\omega+k_3(-\omega e_1+v_r\sin e_3) \quad (14)$$

To stabilize three error variables $e_1(t)$, $e_2(t)$ and $\bar{e}_3(t)$, one proposes the following control laws for v and ω ,

$$\begin{cases} v=\phi_2=k_1e_1+v_r\cos e_3 \\ \omega=\phi_3=\dfrac{1}{1+k_3e_1}\left(k_2\bar{e}_3+v_r\dfrac{\sin e_3}{\bar{e}_3}e_2+\alpha v_r\sin e_3+\omega_r\right) \end{cases} \quad (15)$$

Note that it is easy to show that the set of control laws (15) stabilizes three error variables $e_1(t)$, $e_2(t)$ and $\bar{e}_3(t)$.

3.2.2 Dynamic Level

3.2.2.1 Sliding-Mode Yaw Rate Control

This subsection proposes the sliding-mode yaw rate controller to steer the SBTWR to exactly track the virtual angular velocity command ϕ_3 . The yaw rate controller can be designed based on the following decoupled and simplified yaw motion model

$$\dot{\omega}=f_{23}(x)+(R\cdot b/G_\alpha)C_y$$

Define the sliding surface S_η by

$$S_\eta=\omega-\phi_3 \quad (16)$$

Differentiating S_η gives

$$\dot{S}_\eta=\dot{\omega}-\dot{\phi}_3=f_{23}(x)+(R\cdot b/G_\alpha)C_y-\dot{\phi}_3 \quad (17)$$

The control objective is to find a sliding-mode control law for C_y such that $S_\eta\to 0$ in finite time. Thus, let the yaw rate control law be

$$C_y=\frac{G_\alpha}{R\cdot b}[-f_{23}(x)+\dot{\phi}_3-K_{\eta\omega1}\,\mathrm{sgn}(S_\eta)-K_{\eta\omega2}S_\eta] \quad (18)$$

such that

$$\dot{S}_\eta=-K_{\eta\omega1}\,\mathrm{sgn}(S_\eta)-K_{\eta\omega2}S_\eta, K_{\eta\omega1}>0, K_{\eta\omega2}>0 \quad (19)$$

To show that $S_\eta\to 0$ in finite time, one proposes the Lyapunov function $V_2=S_\eta^{\,2}/2$ whose time derivative is

$$\dot{V}_2=S_\eta\dot{S}_\eta=-K_{\eta\omega1}\left|S_\eta\right|-K_{\eta\omega2}S_\eta^{\,2}\le -K_{\eta\omega1}\left|S_\eta\right| \quad (20)$$

This indicates that $S_\eta\to 0$ in finite time. In practice, the signum function will be replaced by a saturation function to avoid the chattering phenomenon.

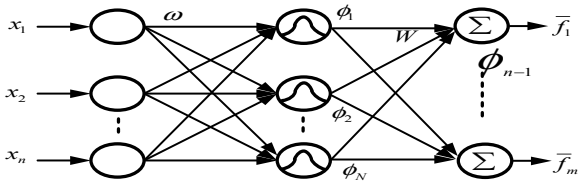

Fig.2. FBFN structure.

3.2.2.2 Aggregate Hierarchical Sliding-Mode Control

The control objective of the subsection is to find a torque control law for C_θ such that the speed of the platform tracks the virtual linear velocity command ϕ_2 without errors, and the tile angle of the platform is maintained at zero simultaneously. In what follows, the aggregate hierarchical sliding-mode control approach in [11] is used to find torque control law for C_θ by using the following simplified and coupled 2-state state equation

$$\begin{bmatrix} \dot{\omega}_\alpha \\ \dot{v} \end{bmatrix} = \begin{bmatrix} f_{21}(\mathbf{x}) \\ f_{22}(\mathbf{x}) \end{bmatrix} + \begin{bmatrix} g_{21}(\mathbf{x}) \\ g_{22}(\mathbf{x}) \end{bmatrix} C_\theta \tag{21}$$

To formulate the hierarchical decoupling sliding-mode controller, one proposes the two first-layer sliding surfaces

$$S_\alpha = \eta_\alpha = \omega_\alpha - \phi_1 = \omega_\alpha - (-K_\alpha \alpha) \tag{22}$$

$$S_v = \eta_v = v - \phi_2 \tag{23}$$

whose time derivatives are respectively given by

$$\dot{S}_\alpha = \dot{\omega}_\alpha + K_\alpha \dot{\alpha} = f_{21}(\mathbf{x}) + g_{21}(\mathbf{x}) C_\theta + K_\alpha \dot{\alpha} \tag{24}$$

$$\dot{S}_v = \dot{v} - \dot{\phi}_2 = f_{22}(\mathbf{x}) + g_{22}(\mathbf{x}) C_\theta - \dot{\phi}_2 \tag{25}$$

Then the second-layer sliding surface is proposed by

$$S_1 = r_1 S_v + r_2 S_\alpha \tag{26}$$

where r_1 and r_2 are two real parameters. To construct the aggregate hierarchical sliding-mode control law [11] such that $S_1, S_v, S_\alpha \to 0$ as $t \to \infty$, one takes the time derivatives of the second-layer sliding surface to be zero, i.e.,

$$\dot{S}_1 = r_1[f_{22}(\mathbf{x}) + g_{22}(\mathbf{x}) C_\theta - \dot{\phi}_2] + r_2(f_{21}(\mathbf{x}) + g_{21}(\mathbf{x}) C_\theta + K_\alpha \dot{\alpha}) \tag{27}$$

The control law for C_θ is chosen by

$$\tau_p = \frac{1}{r_1 g_{21}(\mathbf{x}) + r_2 g_{22}(\mathbf{x})} [-r_1 f_{21}(\mathbf{x}) - r_2 f_{22}(\mathbf{x}) - r_1 k_\alpha \dot{\alpha} + r_2 \dot{\phi}_2 - K_{s1} \operatorname{sgn}(S_1) - K_{s2} S_1], K_{s1} > 0, K_{s2} > 0 \tag{28}$$

which leads to $\dot{S}_1 = -K_{s1} \operatorname{sgn}(S_1) - K_{s2} S_1$. The fact that S_1 approaches zero in finite time can be easily shown by proposing the Lyapunov function $V_3 = S_1^2 / 2$. Hence, it easily implies that $S_1, S_v, S_\alpha \to 0$ in finite time.

IV. ADAPTIVE TRAJETORY TRACKING

This section will develop an adaptive trajectory tracking controllers using FBFN for the SBTWR with unknown parameters, or abrupt parameter variations. The controllers are derived using the Lyapunov stability theory.

4.1 Brief Review of FBFN

As shown in Fig. 2, the architecture of the FBFN can be represented by a three-layer network with Gaussian functions as its activation functions in the hidden layer and weights w_{kj}'s 's connecting hidden layer and output layer. Thus, the output vector of fuzzy basis function network (FBFN) can be expressed as

$$\overline{f}(\mathbf{x}, \mathbf{c}, \boldsymbol{\omega}, \mathbf{W}) = \mathbf{W}^T S(\mathbf{x}, \mathbf{c}, \boldsymbol{\omega}) \tag{29}$$

where $\mathbf{x} = [x_1, x_2, ..., x_n]^T \in \mathbb{R}^n$, $\mathbf{c} = [c_1^T, c_2^T, ..., c_N^T]^T \in \mathbb{R}^{n \times N}$, $\boldsymbol{\omega} = [\omega_1^T, \omega_2^T, ..., \omega_N^T]^T \in \mathbb{R}^{n \times N}$, $\mathbf{c}_j = [c_{j1}, c_{j2}, ..., c_{jn}]^T \in \mathbb{R}^n$, $\boldsymbol{\omega}_j = [\omega_{j1}, \omega_{j2}, ..., \omega_{jn}]^T \in \mathbb{R}^n$, $\mathbf{W}^T = [\omega_{kj}]$ is an $m \times N$ matrix and

$$S(\mathbf{x}, \mathbf{c}, \boldsymbol{\omega}) = [S_1 \quad S_2 \quad \cdots \quad S_N]^T$$

$$= [e^{-[\omega_1^T (x - c_1)]^2} \quad e^{-[\omega_2^T (x - c_2)]^2} \quad \cdots \quad e^{-[\omega_N^T (x - c_N)]^2}]^T$$

By the Stone–Weierstrass theorem, the FBFN can be proven that it is capable of uniformly approximating any real continuous function $\overline{f}(x)$ on a compact set $\mathbf{U}$ to any arbitrary accuracy b_ε, i.e., there exists an ideal FBFN, $\mathbf{W}^T S(\mathbf{x}, \mathbf{c}, \boldsymbol{\omega})$, with ideal parameters, $\mathbf{c}, \boldsymbol{\omega}$, and $\mathbf{W}$ such that $\sup_{x \in \mathbf{U}} \left\| \overline{f}(x) - \mathbf{W}^T S(\mathbf{x}, \mathbf{c}, \boldsymbol{\omega}) \right\| < b_\varepsilon$. Therefore, $\overline{f}(x)$ can be represented as

$$\overline{f}(x) = \mathbf{W}^T S(\mathbf{x}, \mathbf{c}, \boldsymbol{\omega}) + \varepsilon_f \tag{30}$$

where $\left\| \varepsilon_f \right\| \le b_\varepsilon$.

4.2 Adaptive Posture and Speed Control Using FBFN

To develop adaptive sliding-mode posture and speed control law for C_θ, it is necessary to rewrite (28) in the following form

$$C_\theta = -f_p(\mathbf{x}) - K_{SS1} sgn(S_1) - K_{SS2} S_1 \tag{31}$$

where $f_p(\mathbf{x}) = \frac{1}{r_1 g_{22}(\mathbf{x}) + r_2 g_{21}(\mathbf{x})} [-r_1 f_{22}(\mathbf{x}) - r_2 f_{21}(\mathbf{x}) - r_2 K_\alpha \dot{\alpha} + r_1 \dot{\phi}_2]$

$$K_{SS1} = \frac{K_{S1}}{r_1 g_{22}(\mathbf{x}) + r_2 g_{21}(\mathbf{x})}, \quad K_{SS2} = \frac{K_{S2}}{r_1 g_{22}(\mathbf{x}) + r_2 g_{21}(\mathbf{x})}$$

Since the bounded function $f_p(\mathbf{x})$ in (31) can be on-line learned by the FBFN, it is good to propose the following adaptive control

$$C_\theta = -\hat{f}_p(\mathbf{x}) - K_{SS1} sgn(S_1) - K_{SS2} S_1 \tag{32}$$

where $\hat{f}_p$ is the estimate of f_p using the FBFN proposed in Section 4.1, namely that

$$f_p = \mathbf{W_p}^{*T} \boldsymbol{\Phi_p}^* + \varepsilon_p^* = [W_{p1}^* \cdots W_{pn}^*][\Phi^*_{p1} \quad \cdots \quad \Phi^*_{pn}]^T + \varepsilon_p^* \tag{33}$$

and

$$\hat{f}_p = \hat{\mathbf{W}}_\mathbf{p}^T \hat{\boldsymbol{\Phi}}_\mathbf{p} = [\hat{W}_{p1} \cdots \hat{W}_{pn}][\hat{\Phi}_{p1} \quad \cdots \quad \hat{\Phi}_{pn}]^T \tag{34}$$

where

$$\Phi^*_{pi} = \exp\{-[(\alpha - c^*_{p1i})^2 + (\omega_\alpha - c^*_{p2i})^2 + (\dot{\theta} - c^*_{p3i})^2 + (\dot{\phi}_2 - c^*_{p4i})^2] \omega^*_{pi}\} \tag{35}$$

and

$$\hat{\Phi}_{pi} = \exp\{-[(\alpha - \hat{c}_{p1i})^2 + (\omega_\alpha - \hat{c}_{p2i})^2 + (\dot{\theta} - \hat{c}_{p3i})^2 + (\dot{\phi}_2 - \hat{c}_{p4i})^2] \hat{\omega}_{pi}\} \tag{36}$$

Moreover, by defining $\tilde{\mathbf{W}}_\mathbf{p} = \mathbf{W_p}^* - \hat{\mathbf{W}}_\mathbf{p}$, $\tilde{\boldsymbol{\Phi}}_\mathbf{p} = \boldsymbol{\Phi}_\mathbf{p}^* - \hat{\boldsymbol{\Phi}}_\mathbf{p}$, one obtains

$$f_p = \hat{\mathbf{W}}_\mathbf{p}^T \hat{\boldsymbol{\Phi}}_\mathbf{p} + \hat{\mathbf{W}}_\mathbf{p}^T \tilde{\boldsymbol{\Phi}}_\mathbf{p} + \tilde{\mathbf{W}}_\mathbf{p}^T \hat{\boldsymbol{\Phi}}_\mathbf{p} + \tilde{\mathbf{W}}_\mathbf{p}^T \tilde{\boldsymbol{\Phi}}_\mathbf{p} + \varepsilon_p^* \tag{37}$$

In order to achieve on-line tuning of the FBFN parameters, including the center vector $\mathbf{c_p}=[c_{p11}\ c_{p21}\ c_{31}\ c_{41}\ ...\ c_{p1n}\ c_{p2n}\ c_{p3n}\ c_{p4n}]^T$ and the vector $\boldsymbol{\omega}_\mathbf{p}=[\omega_{p1}\ \omega_{p2}\ \omega_{p3}\ ...\ \omega_{pn}]^T$, the expansion of $\tilde{\boldsymbol{\Phi}}_p$ is taken in a Taylor series as follows

$$\tilde{\boldsymbol{\Phi}}_\mathbf{p}=\frac{\partial\tilde{\boldsymbol{\Phi}}_\mathbf{p}}{\partial\hat{\mathbf{C}}_\mathbf{p}}\tilde{\mathbf{C}}_\mathbf{p}+\frac{\partial\tilde{\boldsymbol{\Phi}}_\mathbf{p}}{\partial\hat{\boldsymbol{\omega}}_\mathbf{p}}\tilde{\boldsymbol{\omega}}_\mathbf{p}+\mathbf{h_p}=\mathbf{A_p}\tilde{\mathbf{C}}_\mathbf{p}+\mathbf{B_p}\tilde{\boldsymbol{\omega}}_\mathbf{p}+\mathbf{h_p} \quad (38)$$

where $\tilde{\mathbf{C}}_\mathbf{p}=\mathbf{C}_\mathbf{p}^*-\hat{\mathbf{C}}_\mathbf{p}$; $\tilde{\boldsymbol{\omega}}_\mathbf{p}=\boldsymbol{\omega}_\mathbf{p}^*-\hat{\boldsymbol{\omega}}_\mathbf{p}$; h is the vector containing higher order terms and satisfies $\|\mathbf{h_p}\|\le b$. Substituting (38) into (37) gives

$$f_p=\hat{\mathbf{W}}_\mathbf{p}^T\hat{\boldsymbol{\Phi}}_\mathbf{p}+\hat{\mathbf{W}}_\mathbf{p}^T(\mathbf{A_p}\tilde{\mathbf{C}}_\mathbf{p}+\mathbf{B_p}\tilde{\boldsymbol{\omega}}_\mathbf{p}+h_p)+\tilde{\mathbf{W}}_\mathbf{p}^T\hat{\boldsymbol{\Phi}}_\mathbf{p}+\tilde{\mathbf{W}}_\mathbf{p}^T\tilde{\boldsymbol{\Phi}}_\mathbf{p}+\varepsilon_p^* \quad (39)$$

where $\varepsilon_p=\hat{\mathbf{W}}_\mathbf{p}^T\mathbf{h_p}+\tilde{\mathbf{W}}_\mathbf{p}^T\tilde{\boldsymbol{\Phi}}_\mathbf{p}+\varepsilon_p^*$ and ε_p is assumed to satisfies $|\varepsilon_p|<g_{p\max}$. Substituting the proposed controller (32) into $\dot{S}_1$ in (20) yields

$$\begin{aligned}\dot{S}_1&=[r_1g_{22}(\mathbf{x})+r_2g_{21}(\mathbf{x})]\left[C_\theta+\frac{r_1f_{22}(\mathbf{x})+r_2f_{21}(\mathbf{x})}{r_1g_{22}(\mathbf{x})+r_2g_{21}(\mathbf{x})}+\frac{r_2K_\alpha\alpha-r_1\dot{\phi}_2}{r_1g_{22}(\mathbf{x})+r_2g_{21}(\mathbf{x})}\right]\\&=\Delta_p[-\hat{f}_p-K_{SS1}sgn(S_1)-K_{SS2}S_1+f_p]\\&=\Delta_p[\hat{\mathbf{W}}_\mathbf{p}^T(A_p\tilde{C}_p+B_p\tilde{\omega}_p+h_p)+\tilde{\mathbf{W}}_\mathbf{p}^T\hat{\Phi}_p+\tilde{\mathbf{W}}_\mathbf{p}^T\tilde{\Phi}_p]+\varepsilon_p^*-K_{SS1}sgn(S_1)-K_{SS2}S_1]\end{aligned} \quad (40)$$

where $\varepsilon_p=\tilde{\mathbf{W}}_\mathbf{p}^T\tilde{\boldsymbol{\Phi}}_p+\hat{\mathbf{W}}_\mathbf{p}h_p+\varepsilon_p^*$, $\Delta_p=r_1g_{22}(\mathbf{x})+r_2g_{21}(\mathbf{x})$

Note that Δ_p is made negative if both parameters r_1 and r_2 are properly chosen. Moreover, we have

$$\begin{aligned}S_1\dot{S}_1&=\Delta_p\{S_1[\hat{\mathbf{W}}_\mathbf{p}^T(A_p\tilde{C}_p+B_p\tilde{\omega}_p)+\tilde{\mathbf{W}}_\mathbf{p}^T\hat{\Phi}_p]\}\\&\quad+(-K_{S1}sgn(S_1)-K_{S2}S_1)S_1+\varepsilon_pS_1\}\\&=\Delta_p\{S_1[\hat{\mathbf{W}}_\mathbf{p}^T(A_p\tilde{C}_p+B_p\tilde{\omega}_p)+\tilde{\mathbf{W}}_\mathbf{p}^T\hat{\Phi}_p]-K_{SS1}|S_1|-K_{SS2}S_1^2+\varepsilon_pS_1\}\end{aligned} \quad (41)$$

Using the inequality $A+B\ge A-|B|$, one obtains

$$\begin{aligned}&S_1[\hat{\mathbf{W}}_\mathbf{p}^T(A_p\tilde{C}_p+B_p\tilde{\omega}_p)+\tilde{\mathbf{W}}_\mathbf{p}^T\hat{\Phi}_p]-K_{SS1}|S_1|-K_{SS2}S_1^2+\varepsilon_pS_1\\&\ge S_1[\hat{\mathbf{W}}_\mathbf{p}^T(A_p\tilde{C}_p+B_p\tilde{\omega}_p)+\tilde{\mathbf{W}}_\mathbf{p}^T\hat{\Phi}_p]-K_{SS1}|S_1|-K_{SS2}S_1^2-g_{p\max}|S_1|\end{aligned}$$

where $|\varepsilon_p|\le g_{p\max}$. Since $\Delta_p<0$, one obtains

$$\begin{aligned}S_1\dot{S}_1&\le\Delta_p\{S_1[\hat{\mathbf{W}}_\mathbf{p}^T(A_p\tilde{C}_p+B_p\tilde{\omega}_p)+\tilde{\mathbf{W}}_\mathbf{p}^T\hat{\Phi}_p]-(K_{SS1}+g_{p\max})|S_1|-K_{SS2}S_1^2\}\\&=\Delta_p\{S_1[\hat{\mathbf{W}}_\mathbf{p}^T(A_p\tilde{C}_p+B_p\tilde{\omega}_p)+\tilde{\mathbf{W}}_\mathbf{p}^T\hat{\Phi}_p]\}-(K_{S1}+\Delta_pg_{p\max})|S_1|-K_{S2}S_1^2\end{aligned} \quad (42)$$

Next, move to find the parameter updating laws for $\hat{\mathbf{W}}_\mathbf{p}$, $\hat{\mathbf{C}}_\mathbf{p}$, $\hat{\boldsymbol{\omega}}_\mathbf{p}$. In doing so, the following Lyapunov function candidate is proposed by

$$V_1=\frac{1}{2}S_1^2+\frac{\tilde{\mathbf{C}}_\mathbf{p}^T\tilde{\mathbf{C}}_\mathbf{p}}{2\lambda_{C_p}}+\frac{\tilde{\boldsymbol{\omega}}_\mathbf{p}^T\tilde{\boldsymbol{\omega}}_\mathbf{p}}{2\lambda_{C_p}}+\frac{\tilde{\mathbf{W}}_\mathbf{p}^T(-\dot{\hat{\mathbf{W}}}_\mathbf{p})}{2\lambda_{w_p}} \quad (43)$$

which leads to

$$\begin{aligned}\dot{V}_1&\le\tilde{C}_p\mathbf{A_p}^T\hat{\mathbf{W}}_\mathbf{p}S_1\Delta_p+\tilde{\boldsymbol{\omega}}_\mathbf{p}^T\mathbf{B_p}^T\hat{\mathbf{W}}_\mathbf{p}S_1\Delta_p+\tilde{\mathbf{W}}_\mathbf{p}^T\hat{\boldsymbol{\Phi}}_\mathbf{p}\Delta_pS_1-(K_{S1}+\Delta_pg_{p\max})|S_1|\\&\quad-K_{S2}S_1^2+\frac{\tilde{\mathbf{C}}_\mathbf{p}^T}{\lambda_{C_p}}(-\dot{\hat{\mathbf{C}}}_\mathbf{p})+\frac{\tilde{\boldsymbol{\omega}}_\mathbf{p}^T}{\lambda_{\omega_p}}(-\dot{\hat{\boldsymbol{\omega}}}_\mathbf{p})+\frac{\tilde{\mathbf{W}}_\mathbf{p}^T}{\lambda_{W_p}}(-\dot{\hat{\mathbf{W}}}_\mathbf{p})\\&=-(K_{S1}+\Delta_pg_{p\max})|S_1|-K_{S2}S_1^2+\tilde{\mathbf{W}}_\mathbf{p}^T[-\frac{\dot{\hat{\mathbf{W}}}_\mathbf{p}}{\lambda_{W_p}}+\hat{\boldsymbol{\Phi}}_\mathbf{p}\Delta_pS_1]\\&\quad+\tilde{\mathbf{C}}_\mathbf{p}^T[-\frac{\dot{\hat{\mathbf{C}}}_\mathbf{p}}{\lambda_{C_p}}+\mathbf{A_p}^T\hat{\mathbf{W}}_\mathbf{p}S_1\Delta_p]+\tilde{\boldsymbol{\omega}}_\mathbf{p}^T[-\frac{\dot{\hat{\boldsymbol{\omega}}}_\mathbf{p}}{\lambda_{W_p}}+\mathbf{B_p}^T\hat{\mathbf{W}}_\mathbf{p}S_1\Delta_p]\end{aligned} \quad (44)$$

Let the parameter adjustment rules be chosen by

$$\dot{\hat{\mathbf{W}}}_\mathbf{p}=\lambda_{W_p}\Delta_p\hat{\boldsymbol{\Phi}}_\mathbf{p}S_1,\dot{\hat{\mathbf{C}}}_\mathbf{p}=\lambda_{C_p}\mathbf{A_p}^T\hat{\mathbf{W}}_\mathbf{p}S_1\Delta_p,\dot{\hat{\boldsymbol{\omega}}}_\mathbf{p}=\lambda_{\omega_p}\mathbf{B_p}^T\hat{\mathbf{W}}_\mathbf{p}S_1\Delta_p \quad (45)$$

Thus, if $K_{S1}+\Delta_pg_{p\max}>0$, then

$$\dot{V}\le-(K_{S1}+\Delta_pg_{p\max})|S_1|-K_{S2}S_1^2\le0 \quad (46)$$

which implies $S_1\to0$ in finite time.

4.3 Adaptive Yaw Rate Control Using FBFN

Similarly,the sliding-mode control law (18) can be rewritten by

$$C_y=-f_y(\mathbf{x})-\frac{G_\alpha K_{\eta w1}}{R\cdot b}\mathrm{sgn}(S_\eta)-\frac{G_\alpha K_{\eta w2}}{R\cdot b}S_\eta \quad (47)$$

where $f_y(x)=G_\alpha f_{23}(\mathbf{x})/R\cdot b-G_\alpha\dot{\phi}_3/(R\cdot b)$. Hence, the proposed adaptive yaw rate controller is expressed by

$$C_y=-\hat{f}_y(\mathbf{x})-[K_6+g_y]\mathrm{sgn}(S_\eta)\ ,\ g_y\ge g_{y\max},\ K_6>0 \quad (48)$$

where $\hat{f}_y$ is the estimate of f_y using the FBFN proposed in Section4.1, namely that

$$f_y=\mathbf{W}_y^{*T}\boldsymbol{\Phi}_y^*+\varepsilon_y^*=[W_{y1}^*\cdots W_{ym}^*][\Phi_{y1}^*\ \cdots\ \Phi_{ym}^*]^T+\varepsilon_y^* \quad (49)$$

$$\hat{f}_y=\hat{\mathbf{W}}_y^T\hat{\boldsymbol{\Phi}}_y=[\hat{W}_{y1}\cdots\hat{W}_{ym}][\hat{\Phi}_{y1}\ \cdots\ \hat{\Phi}_{ym}]^T \quad (50)$$

where

$$\boldsymbol{\Phi}_{yi}^*=\exp\{-[(\alpha-c_{y1i}^*)^2+(\omega_\alpha-c_{y2i}^*)^2+(\dot{\theta}-c_{y3i}^*)^2+(v-c_{y4i}^*)^2+(\dot{\phi}_3-c_{y5i}^*)^2]\omega_{yi}^*\} \quad (51)$$

$$\hat{\boldsymbol{\Phi}}_{yi}=\exp\{-[(\alpha-\hat{c}_{y1i})^2+(\omega_\alpha-\hat{c}_{y2i})^2+(\dot{\theta}-\hat{c}_{y3i})^2+(v-\hat{c}_{y4i})^2+(\dot{\phi}_3-\hat{c}_{y5i})^2]\hat{\omega}_{yi}\} \quad (52)$$

Similarly, by defining $\tilde{\mathbf{W}}_y=\mathbf{W}_y^*-\hat{\mathbf{W}}_y$, $\tilde{\boldsymbol{\Phi}}_y=\boldsymbol{\Phi}_y^*-\hat{\boldsymbol{\Phi}}_y$, one obtains

$$f_y=\hat{\mathbf{W}}_y^T\hat{\boldsymbol{\Phi}}_y+\hat{\mathbf{W}}_y^T\tilde{\boldsymbol{\Phi}}_y+\tilde{\mathbf{W}}_y^T\hat{\boldsymbol{\Phi}}_y+\tilde{\mathbf{W}}_y^T\tilde{\boldsymbol{\Phi}}_y+\varepsilon_y^* \quad (53)$$

In order to achieve on-line tuning of the FBFN parameters, including the center vector $\mathbf{C}_y=[c_{y11}\ c_{y21}\ c_{y31}\ ...\ c_{y1n}\ c_{y2n}\ c_{y3n}]^T$ and the vector $\boldsymbol{\omega}_y=[\omega_{y1}\ \omega_{y2}\ \omega_{y3}\ ...\ \omega_{ym}]^T$, the expansion of $\tilde{\boldsymbol{\Phi}}_y$ is taken in a Taylor series as follows:

$$\tilde{\boldsymbol{\Phi}}_\mathbf{y}=\frac{\partial\tilde{\boldsymbol{\Phi}}_y}{\partial\hat{\mathbf{C}}_y}\tilde{\mathbf{C}}_y+\frac{\partial\tilde{\boldsymbol{\Phi}}_y}{\partial\hat{\boldsymbol{\omega}}_y}\tilde{\boldsymbol{\omega}}_y+\mathbf{h}_y=\mathbf{A}_y\tilde{\mathbf{C}}_y+\mathbf{B}_y\tilde{\boldsymbol{\omega}}_y+\mathbf{h}_y \quad (54)$$

where $\tilde{\mathbf{C}}_y=\mathbf{C}_y^*-\hat{\mathbf{C}}_y$; $\tilde{\boldsymbol{\omega}}_y=\boldsymbol{\omega}_y^*-\hat{\boldsymbol{\omega}}_y$; h_p is the vector containing higher order terms and satisfies $\|h_y\|\le b$. Substituting (54) into (53) gives

$$f_y=\hat{\mathbf{W}}_y^T\hat{\boldsymbol{\Phi}}_y+\hat{\mathbf{W}}_y^T(\mathbf{A}_y\tilde{\mathbf{C}}_y+\mathbf{B}_y\tilde{\boldsymbol{\omega}}_y+h_y)+\tilde{\mathbf{W}}_y^T\hat{\boldsymbol{\Phi}}_y+\tilde{\mathbf{W}}_y^T\tilde{\boldsymbol{\Phi}}_y+\varepsilon_y^* \quad (55)$$

where $\varepsilon_y=\hat{\mathbf{W}}_y^T\mathbf{h}_y+\tilde{\mathbf{W}}_y^T\tilde{\boldsymbol{\Phi}}_y+\varepsilon_y^*$ and $\boldsymbol{\varepsilon}$ is assumed to satisfies $|\varepsilon_y|<g_{y\max}$ .Substituting C_y in (48) into $\dot{S}_\eta$ in (17) gives

$$\begin{aligned}\dot{S}_\eta&=f_{23}(x)+\frac{R\cdot b}{G_\alpha}C_y-\dot{\phi}_3=\frac{R\cdot b}{G_\alpha}[C_y+f_y]\\&=\frac{R\cdot b}{G_\alpha}[f_y-\hat{f}_y+[-K_6-g_y]\mathrm{sgn}(S_\eta)]\\&=\frac{R\cdot b}{G_\alpha}[\hat{\mathbf{W}}_\mathbf{y}^T(A_y\tilde{C}_y+B_y\tilde{\omega}_y)+\tilde{\mathbf{W}}_\mathbf{y}^T\hat{\boldsymbol{\Phi}}_\mathbf{y}+\varepsilon_y+(-K_6-g_y)\mathrm{sgn}(S_\eta)]\end{aligned} \quad (56)$$

where

$$\varepsilon_y=\tilde{\mathbf{W}}_\mathbf{y}^T\tilde{\boldsymbol{\Phi}}_\mathbf{y}+\hat{\mathbf{W}}_\mathbf{y}^Th_y+\varepsilon_y^*\ ,\ \Delta_y=R\cdot b/G_\alpha>0$$

and

$$S_\eta\dot{S}_\eta=\Delta_y[\hat{\mathbf{W}}_\mathbf{y}^T((\mathbf{A_y}\tilde{\mathbf{C}}_\mathbf{y}+\mathbf{B_y}\tilde{\boldsymbol{\omega}}_\mathbf{y})+\tilde{\mathbf{W}}_\mathbf{y}^\mathbf{T}\hat{\boldsymbol{\Phi}}_\mathbf{y})S_\eta+(-K_6-g_y)|S_\eta|+\varepsilon_yS_\eta]$$

using the inequality $A+B\le A+|B|$

$$
\begin{aligned}
S_\eta \dot{S}_\eta &\le \Delta_y\{\hat{\mathbf{W}}_\mathbf{y}^{\mathrm{T}}((\mathbf{A}_\mathbf{y}\tilde{\mathbf{C}}_\mathbf{y}+\mathbf{B}_\mathbf{y}\tilde{\boldsymbol{\omega}}_\mathbf{y})+\tilde{\mathbf{W}}_\mathbf{y}^{\mathrm{T}}\hat{\boldsymbol{\Phi}}_\mathbf{y})S_\eta+(-K_6-g_y)|S_\eta|+|\varepsilon_y||S_\eta|\} \\
&\le \Delta_y\{[\hat{\mathbf{W}}_\mathbf{y}^{\mathrm{T}}(\mathbf{A}_\mathbf{y}\tilde{\mathbf{C}}_\mathbf{y}+\mathbf{B}_\mathbf{y}\tilde{\boldsymbol{\omega}}_\mathbf{y})+\tilde{\mathbf{W}}_\mathbf{y}^{\mathrm{T}}\hat{\boldsymbol{\Phi}}_\mathbf{y}]S_\eta-(g_y-g_{y\max})|S_\eta|-K_6|S_\eta|\} \\
&\le \Delta_y\{[\hat{\mathbf{W}}_\mathbf{y}^{\mathrm{T}}(\mathbf{A}_\mathbf{y}\tilde{\mathbf{C}}_\mathbf{y}+\mathbf{B}_\mathbf{y}\tilde{\boldsymbol{\omega}}_\mathbf{y})+\tilde{\mathbf{W}}_\mathbf{y}^{\mathrm{T}}\hat{\boldsymbol{\Phi}}_\mathbf{y}]S_\eta-K_6|S_\eta|\}
\end{aligned} \quad (57)
$$

which $|\varepsilon_y| < g_{ymax}$. To obtain the parameter updating rules for $\hat{W}_y$, $\hat{C}_y$, $\hat{\omega}_y$, we have

$$
V_2 = \frac{1}{2}S_\eta^{\,2} + \frac{\tilde{\mathbf{W}}_\mathbf{y}^{\,T}\tilde{\mathbf{W}}_\mathbf{y}}{2\lambda_{W_y}} + \frac{\tilde{\mathbf{C}}_\mathbf{y}^{\,T}\tilde{\mathbf{C}}_\mathbf{y}}{2\lambda_{C_y}} + \frac{\tilde{\boldsymbol{\omega}}_\mathbf{y}^{\,T}\tilde{\boldsymbol{\omega}}_\mathbf{y}}{2\lambda_{\omega_y}} \quad (58)
$$

Taking the time derivative of V_2 gives

$$
\begin{aligned}
\dot{V}_2 = {} & S_\eta\dot{S}_\eta + \frac{\tilde{\mathbf{W}}_\mathbf{y}^{\,T}}{\lambda_{W_y}}(-\dot{\hat{\mathbf{W}}}_y) + \frac{\tilde{\mathbf{C}}_\mathbf{y}^{\,T}}{\lambda_{C_y}}(-\dot{\hat{\mathbf{C}}}_y) + \frac{\tilde{\boldsymbol{\omega}}_\mathbf{y}^{\,T}}{\lambda_{\omega_y}}(-\dot{\hat{\boldsymbol{\omega}}}_\mathbf{y}) \\
\le {} & -K_6\Delta_y|S_\eta| + \tilde{\mathbf{W}}_\mathbf{y}^{\,T}[-\frac{\dot{\hat{\mathbf{W}}}_\mathbf{y}}{\lambda_{W_y}} + \Delta_y\hat{\boldsymbol{\Phi}}_\mathbf{y}S_\eta] + \tilde{\mathbf{C}}_\mathbf{y}^{\,T}[-\frac{\dot{\hat{\mathbf{C}}}_\mathbf{y}}{\lambda_{C_y}} + \mathbf{A}_\mathbf{y}^{\,T}\hat{W}_y\Delta_y S_\eta] \\
& + \tilde{\boldsymbol{\omega}}_\mathbf{y}^{\,T}[-\frac{\dot{\hat{\boldsymbol{\omega}}}_\mathbf{y}}{\lambda_{\omega_y}} + \mathbf{B}_\mathbf{y}^{\,T}\hat{\mathbf{W}}_\mathbf{y}\Delta_y S_\eta]
\end{aligned} \quad (59)
$$

If the parameter updating rules are selected as

$$
\dot{\hat{\mathbf{W}}}_y = \lambda_{W_y}\Delta_y\hat{\boldsymbol{\Phi}}_y S_\eta, \dot{\hat{\mathbf{C}}}_y = \lambda_{C_y}\mathbf{A}_\mathbf{y}^{\,T}\hat{\mathbf{W}}_\mathbf{y}\Delta_y S_\eta, \dot{\hat{\boldsymbol{\omega}}}_\mathbf{y} = \lambda_{\omega_y}\mathbf{B}_\mathbf{y}^{\,T}\hat{\mathbf{W}}_\mathbf{y}\Delta_y S_\eta \quad (60)
$$

Then $\dot{V}_2 \le -K_6\Delta_y|S_\eta|$ and, thus, it implies that $S_\eta \to 0$ in finite time.

V. SIMULATIONS AND DISCUSSION

In the section, two simulations are conducted to examine the effectiveness and merit of the proposed adaptive controllers using FBFN. The parameters of the SBTWR are given in Table 1, and the parameters of the virtual trajectory generator in the kinematic level are k_3=0.75; k_1=0.2 , k_2=0.3. The controller's parameters of the proposed adaptive controller using FBFNs are respectively given by $\lambda_{W_p}=0.04$, $\lambda_{C_p}=0.04$, $\lambda_{\omega_p}=0.04$, $\lambda_{W_y}=0.01$, $\lambda_{C_y}=0.01$, $\lambda_{\omega_y}=0.01$, and the initial values of W_p and W_y are 0.0012, 0.0077, respectively. Furthermore, r_1=1, r_2=0.35, $K_{\eta\omega 1}=K_{\eta\omega 2}$=10, $K_{s1}=K_{s2}$=10, and K_α=2.0. Figs. 3-4 present the simulated results of the proposed adaptive controller for tracking a straight line and a circle. The results in Figs. 3-4 indicate that the proposed adaptive control method tracked both trajectories well.

V. CONCLUSIONS

The paper has presented adaptive sliding-mode trajectory tracking controller using FBFN method for posture and yaw control of the SBTWR in presence of parameter variations and model uncertainties. The FBFN has been used to compensate for the effects of the model uncertainties and parameter variations. The adaptive control laws have been employed to overcome the performance degradation caused by parameter variations. Through simulation results, the two proposed adaptive control laws using FBFNs have been shown capable of achieving trajectory tracking. An interesting future work would be to investigate the regulation problem of the SBTWR.

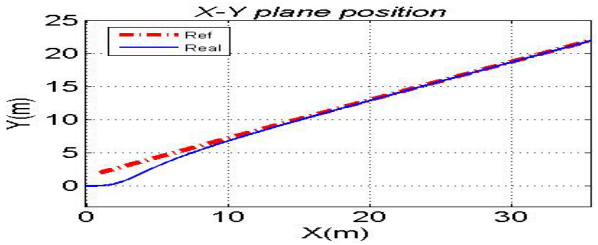

Fig.3. Simulation result of the proposed adaptive tracking controller for line trajectory tracking.

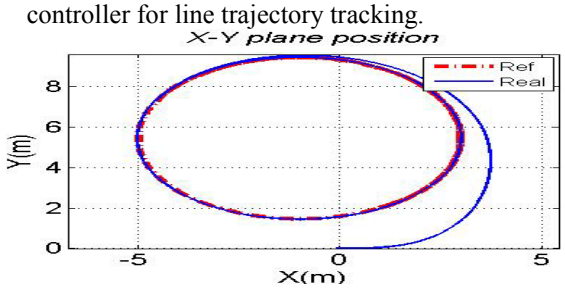

Fig.4. Simulation result of the proposed adaptive tracking controller for circular trajectory tracking using FBFN.

REFERENCES

[1] D. Voth, "Segway to the future," *Intelligent Systems, IEEE [see also IEEE Intelligent Systems and Their Applications]* vol.20, no.3, pp.5 – 8, May-June 2005.

[2] Y.Hosoda, S. Egawa, J. Tamamoto, K. Yamamoto, R.Nakamura and M.Togami "Basic design of human-symbiotic robot EMIEW," in *Pro. IEEE/RSJ International Conference on Intelligent Robots and Systems*, Beijing, China, pp.5079-5084, Oct. 9 - 15, 2006.

[3] C. C. Tsai, H. C. Huang, S. C. Lin, " Adaptive Neural Network Control of a Self-balancing Two-wheeled Scooter," *IEEE Transactions on Industrial Electronics,* vol. 57, no. 4, pp.1420-1428, April 2010.

[4] M. Sasaki, N. Yanagihara, O. Matsumoto, and K. Komoriya, "Steering control of the personal riding-type wheeled mobile platform (PMP)," in *Proc. 2005 IEEE International Conference on Intelligent Robots and Systems*, pp.1697-1702, 2005.

[5] F. Grasser, A.D'Arrigo, and S. Colombi, "JOE: A Mobile, Inverted Pendulum," *IEEE Trans. Industrial Electronics*, vol.49, no.1, pp.107-114, February 2002.

[6] K. Pathak, J. Franch, and S. K. Agrawal, "Velocity and position control of a wheeled inverted pendulum by partial feedback linearization," *IEEE Transactions on* Robotics, vol.21, no.3, pp.505-513, June 2005.

[7] Y.-S. Ha, S. Yuta, "Trajectory tracking control for navigation of the inverse pendulum type self-contained mobile robot," *Robotics and Autonomous Systems*, vol.17, pp. 65-80, 1996.

[9] A. Salerno, and J. Angeles, "The control of semi-autonomous two-wheeled robots undergoing large payload-variations," in *Proc. ICRA'04*, vol.2, pp.1740-1745, Apr 26-May 1, 2004.

[10] C. M. Lin and Y.J. Mon, "Decoupling Control by hierarchical fuzzy sliding-mode controller," *IEEE Transactions on Control System Technology*, vol. 13, no. 4, pp. 593-598, July 2005.

[11] W. Wang, X.D. Liu and J. Q. Yi, "Structure design of two types of sliding-mode controllers for a class of under-actuated mechanical systems," *IET Proceeding of Control Theory and Applications,* vol.1, no.1, pp. 163-172, Jan. 2007.

[12] C. K. Lin, S. D.Wang, "Robust self-tuning rotated fuzzy basis function controller for robot arms," *Control Theory and Applications, IEE Proceedings*, vol.144, no.4, pp.293-298, July 1997.

[13] Z. Huaguang, L. Cai, B. Zeungnam , "A fuzzy basis function vector-based multivariable adaptive controller for nonlinear systems." *IEEE Transactions on Systems, Man, and Cybernetics, Part B,* vol. 30 no.1, pp.210-217, Feb. 2000.

[14] C. K. Lin, "Adaptive critic autopilot design of Bank-to-turn missiles using fuzzy basis function networks," *IEEE Transactions on Systems, Man, and Cybernetics, Part B,* vol. 35 no.2, pp.197-207, April 2005.